frontiers | Frontiers in Earth Science

TYPE Original Research
PUBLISHED 01 November 2023
DOI 10.3389/feart.2023.1280857

Check for updates

OPEN ACCESS

EDITED BY
Yong Wang,
Southwest Petroleum University, China

REVIEWED BY
Xuelong Li,
Shandong University of Science and Technology, China
Qidong Gao,
Chang'an University, China
Geng Jiabo,
Jiangxi University of Science and Technology, China

*CORRESPONDENCE
Wei Zhou,
hnminezhouwei@163.com

RECEIVED 21 August 2023
ACCEPTED 20 October 2023
PUBLISHED 01 November 2023

CITATION
Meng J, Jiao X, Gao S, Zhu X, Cheng S and Zhou W (2023), Study on mechanical and energy characteristics of coal samples under different unloading states. *Front. Earth Sci.* 11:1280857. doi: 10.3389/feart.2023.1280857

COPYRIGHT
© 2023 Meng, Jiao, Gao, Zhu, Cheng and Zhou. This is an open-access article distributed under the terms of the Creative Commons Attribution License (CC BY). The use, distribution or reproduction in other forums is permitted, provided the original author(s) and the copyright owner(s) are credited and that the original publication in this journal is cited, in accordance with accepted academic practice. No use, distribution or reproduction is permitted which does not comply with these terms.

Study on mechanical and energy characteristics of coal samples under different unloading states

Jianbing Meng[1], Xianjun Jiao[2], Song Gao[3], Xiangbin Zhu[3], Shuangli Cheng[3] and Wei Zhou[4]*

[1]School of Safety Science and Engineering, Anhui University of Science and Technology, Huainan, Anhui, China, [2]Huaihe Energy Holding Group Co., Ltd., Huainan, Anhui, China, [3]Huaihe Energy Western Coal Power Group Co., Ltd., Ordos City, China, [4]Pingan Coal Mine Gas Control National Engineering Research Center Co., Ltd., Huainan, Anhui, China

There are many types of coal seams in China, and the mining of protective layers will cause different rates of stress reduction in protected coal seams at different intervals. Therefore, experiments were conducted at different unloading rates to explore the strength, deformation, and energy characteristics of coal. Research findings: the AE (acoustic emission) signal of the coal body before unloading has a small range of changes and similar characteristics. After unloading begins, because of the different development rates of internal crack in the coal body under different unloading states, the AE signal of the coal body varies at different unloading rates. The maximum stress increases exponentially with the increase of unloading rate. It was found that the higher the unloading rate, the easier and earlier the coal sample is to be damaged. And it was discovered that the dissipated energy of the coal sample in the elastic stage is extremely low, and a large amount of total energy is converted into elastic energy and stored inside the coal sample. The dissipation energy increases during the plastic stage, while the trend of increasing elastic energy slows down. After the peak stage, the dissipated energy rapidly increases and the elastic energy decreases.

KEYWORDS

underground engineering, rate of unloading confining pressure, AE signal, peak intensity, energy

1 Introduction

With the development of large-scale underground engineering, the original stress of the rock mass is destroyed during the construction process (Du F. et al., 2022a; Du X. H. et al., 2022b; Li et al., 2022; Liu et al., 2022; Qi et al., 2022; Xie et al., 2022a; 2022b). Rapid excavation will cause an increase in unloading rate, thus causing disasters and accidents occur frequently (Karim and Yamazaki, 2001; Xie et al., 2004; Wang et al., 2022; Zhang et al., 2023). Actually, the failure of rock mass is a process of energy conversion. The deformation mode of coal mass is closely related to energy transformation, and its energy evolution characteristics can truly reflect the deformation process of coal mass (Chen et al., 2014; Cong et al., 2016; Liu S. M. et al., 2023a; Li et al., 2023b). Therefore, it is necessary to study the mechanical and energy characteristics of coal sample failure process under different unloading states.

Various researches in related fields have been reported. For example, the mechanical properties of the selected samples were tested by Triaxial shear test (Peng et al., 2015; Yang, 2016; Chen et al., 2021; Wang and Gao, 2022), which obtained its properties under specific

conditions; In practical engineering, the rock mass is usually in three unequal stress combinations. Therefore, many scholars have also carried out researches on the mechanical properties (Li et al., 2019; Yin et al., 2019), deformation characteristics (Yin et al., 2018; Zhang et al., 2019) and energy characteristics (Luo et al., 2019; Su et al., 2019; Ding et al., 2022) of the samples under the true triaxial test conditions. Among them, (Liu et al., 2019; Liu and Zhao, 2021), studied the dynamic mechanics and failure characteristics of sandstone, then obtained the stress-strain curve and body stress-strain relationship of sandstone in three directions of *X*, *Y* and *Z*-axes under true dynamic triaxial loading, and analyzed the deformation characteristics of sandstone under static-dynamic multi-axial loading by using the world's first system based on true triaxial static load - Triaxial hopkinson bar at Monash University in Australia. Some scholars have also studied the properties of coal under complex conditions from a microscopic perspective (Liu and Li, 2022; Liu H. M. et al., 2023). In the actual engineering, the unloading rate will change with the change of excavation under different unloading paths (Yang et al., 2012; Zhao et al., 2015; Li et al., 2016; Li D. et al., 2017) and different unloading rates (Li X. et al., 2017; Zheng et al., 2017; Ma et al., 2019; Wang et al., 2019), providing references for actual engineering.

In summary, through a lot of research, scholars have achieved fruitful results. However, the site environment and the coal mass are complex and variable (Luo et al., 2019; Chi et al., 2021; Ma et al., 2022; Zhang et al., 2022). However, as the depth of coal mining deepens, the number of multiple coal seams is increasing. And the mining of protected coal seams will cause stress reduction in the protected coal seams, and the closer the distance, the faster the stress reduction. The farther the distance, the slower the rate of stress reduction. It is necessary further to improve on mechanical and energy variation feature of coal samples under different unloading rates. This paper systematically studied the strength, deformation, confining pressure ratio, stabilization time, acoustic emission ring count rate, energy source and direction of coal body under different unloading rates. The research results can provide reference for a deeper understanding of coal mine power disasters.

2 Experiment procedure

2.1 Basic physical parameters of coal body

The coal body came from a coal mine in Shanxi Province, China. Firstly, a number of cuboid shaped coal blocks are taken from the coal mine. Then, a coal sample was drilled from the coal block by a rock drilling machine. Finally, the two ends of the coal samples were polished to obtain a standard coal sample. The length, diameter and quality of the coal sample were measured by vernier caliper and high-precision electronic scale, and the coal sample information is shown in Table 1.

2.2 Experimental method

The rock triaxial testing machine selected for the experiment consists of five parts: control system, load frame device, pore pressure system, confining pressure system, and pressure

TABLE 1 Coal sample information.

Unloading pressure rate (MPa/s)	Numbering	Height (mm)	Diameter (mm)	Quality (g)
0	ANT-11	100.02	50.00	255.25
	ANT-12	100.10	49.98	254.56
	ANT-13	100.12	50.02	255.69
0.02	ANT-21	99.96	50.03	256.04
	ANT-22	100.09	50.06	254.88
	ANT-23	99.91	49.95	255.66
0.04	ANT-31	99.93	49.99	255.33
	ANT-32	99.92	50.01	255.45
	ANT-33	100.23	50.04	254.96
0.06	ANT-41	100.11	50.02	254.84
	ANT-42	99.93	49.96	255.36
	ANT-43	99.99	49.95	255.86
0.08	ANT-51	100.12	50.10	254.91
	ANT-52	100.03	50.06	254.62
	ANT-53	99.96	49.92	255.55
0.10	ANT-61	99.91	49.94	256.12
	ANT-62	99.89	50.06	255.33
	ANT-63	100.11	50.08	255.82

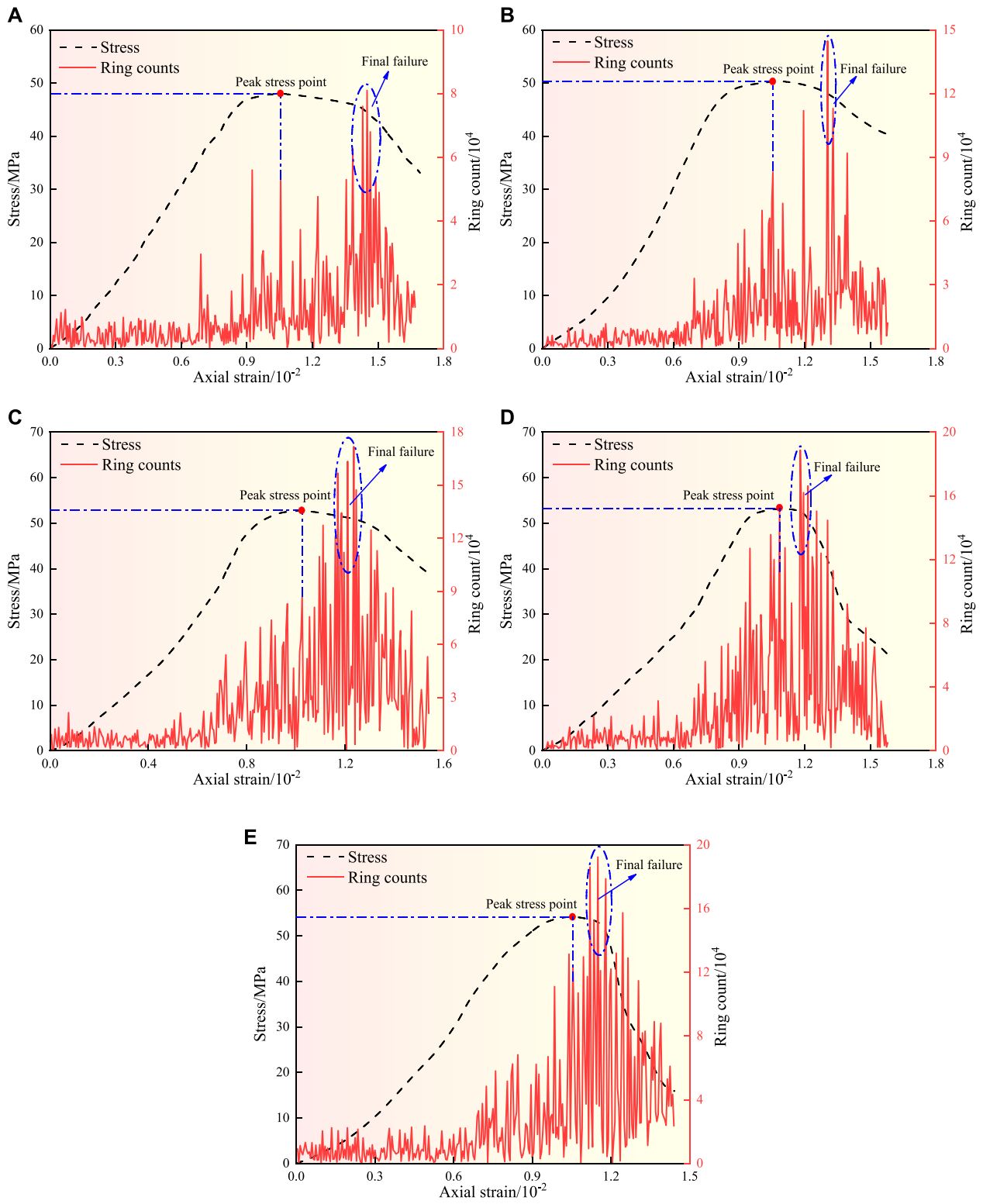

FIGURE 1
Relationship between stress and AE ringing count with axial strain: **(A)** V_1 = 0.02 MPa/s; **(B)** V_2= 0.04 MPa/s; **(C)** V_3 = 0.06 MPa/s; **(D)** V_4= 0.08 MPa/s; **(E)** V_5= 0.1 MPa/s.

chamber, and is equipped with digital voltage servo function. The maximum test force is 5,000 kN, with an error range of ±1%; The maximum confining pressure is 100 MPa, with an error range of ±1%. Due to the experimental conditions, the vertical and horizontal ground stresses at the study site are both 10 MPa.

Conventional triaxial test: apply axial and circumferential stresses to 10 MPa, stabilize the pressure for a certain period of time, and then maintain the circumferential pressure unchanged. Apply axial pressure at a rate of 0.002 mm/s until the sample is damaged.

Unloading confining pressure test: apply axial and circumferential stresses to 10 MPa and maintain stability for a certain period of time. Then apply axial stress to 80% of the ultimate strength of the coal sample and stabilize the pressure, unloading the confining pressure at different rates until the coal sample was destroyed. The rate of unloading confining pressure during the experiment is as follows: V_1=0.02 MPa/s, V_2=0.04 MPa/s, V_3=0.06 MPa/s, V_4=0.08 MPa/s and V_5=0.10 MPa/s.

3 Results

3.1 Strain-stress curve

During the compression of coal samples, there are certain changes in stress and displacement, generated elastic waves. The elastic waves are received by the AE system and converted into AE signals. During the experiment, the stress and AE characteristics of the coal body are shown in Figure 1.

From Figure 1, find out the range of AE signal changes before coal sample unloading is small, and the change characteristics are similar. After the unloading begins, there is a significant difference in the AE signal compared to the loading period, and the AE signal of the coal body also varies significantly at different unloading rates. Simultaneously, it was found that there were differences in the maximum stress of coal body under different unloading rates.

The stress-strain curve has successively undergone four stages: compaction phase, elastic phase, plastic phase and post failure stage. The main stress difference will drop sharply when unloading to a certain extent, which indicates that the coal sample has lost its bearing capacity at this moment, and the destruction of the coal body occurs instantaneously at this moment. The maximum principal stress difference and peak axial strain of coal body under five unloading pressure rates are also different.

In fact, when the unloading rate changes, the degree of deformation of the coal sample will also change, and there are certain differences. When the unloading rate is relatively low, the coal sample deforms fully, and the energy accumulated inside will be slowly released to the outside world; When the unloading rate is relatively high, the damage of the coal sample is sudden, and the energy will be released instantly. This process is relatively dangerous, and should be noted and avoided in practical engineering.

The maximum stress and AE ringing count of coal body under five unloading rates are not acceptable, and their changing states are shown in Figure 2.

V_1 = 0.02 MPa/s, the peak stress is 47.98 MPa; V_2 = 0.04 MPa/s, the peak stress is 4.96% higher than that of the coal sample with a unloading rate of 0.02 MPa/s; V_3 = 0.06 MPa/s, the peak stress is 9.94% higher than the coal sample with a unloading rate of 0.02 MPa/s; V_4 = 0.08 MPa/s, the peak stress is 11.00% higher than the coal sample with a unloading rate of 0.02 MPa/s; V_5 = 0.10 MPa/s, the peak stress is 13.30% higher than the coal sample with a unloading rate of 0.02 MPa/s; In summary, the maximum

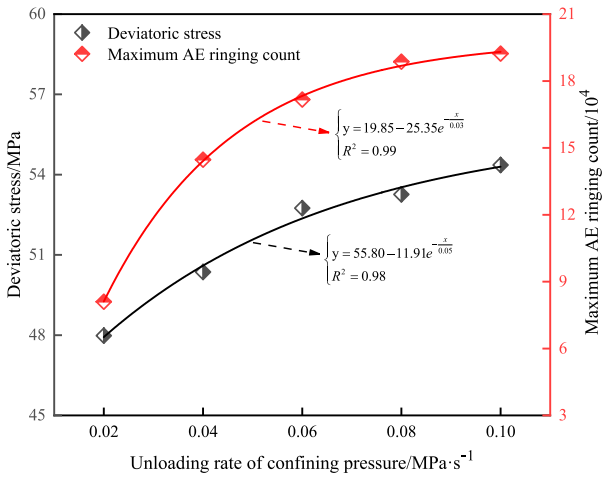

FIGURE 2
The variation trend of maximum stress and AE ringing count.

stress increases with the increase of unloading rate. The relationship between the maximum stress of coal samples and the rate of unloading confining pressure is as follows:

$$\begin{cases} y = 55.80 - 11.91e^{-\frac{x}{0.05}} \\ R^2 = 0.98 \end{cases} \quad (1)$$

V_1 = 0.02 MPa/s, the maximum AE ringing count is 8.1 × 10^4; V_2 = 0.04 MPa/s, the maximum AE ringing count is 78.64% higher than the coal sample with a unloading rate of 0.02 MPa/s; V_3 = 0.06 MPa/s, the maximum AE ringing count is 111.98% higher than that of the coal sample with a unloading rate of 0.02 MPa/s; V_4 = 0.08 MPa/s, the maximum AE ringing count is 132.96% higher than that of the coal sample with a unloading rate of 0.02 MPa/s; V_5 = 0.10 MPa/s, the maximum AE ringing count is 137.41% higher than that of the coal body with a unloading rate of 0.02 MPa/s; In summary, the maximum number of acoustic emission ringing increases with the increase of unloading rate. The relationship between the two is as follows:

$$\begin{cases} y = 19.85 - 25.35e^{-\frac{x}{0.03}} \\ R^2 = 0.99 \end{cases} \quad (2)$$

3.2 Analysis of confine pressure ratios of coal samples

The confining pressure values during coal sample failure vary under different unloading rates. The confining pressure ratio (the ratio of the confining pressure value during coal sample failure to the initial confining pressure) is used to characterize the characteristics of coal sample failure during unloading, as shown in Figure 3.

As shown in Figure 3, as the rate of unloading increases, the confining pressure ratio of the coal body continuously decreases. The confining pressure ratio of coal body with V_2 = 0.04 MPa/s decreased by 10.14% compared to coal body with V_1 = 0.02 MPa/s. The confining pressure ratio of coal body with V_3 = 0.06 MPa/s

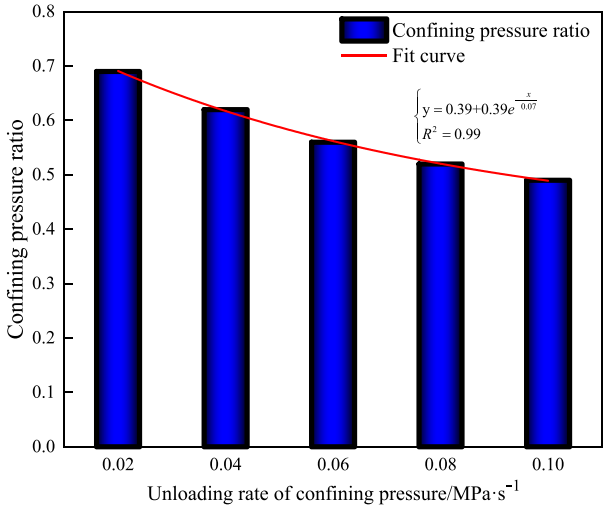

FIGURE 3
Change trend of confining pressure ratio under different unloading rates.

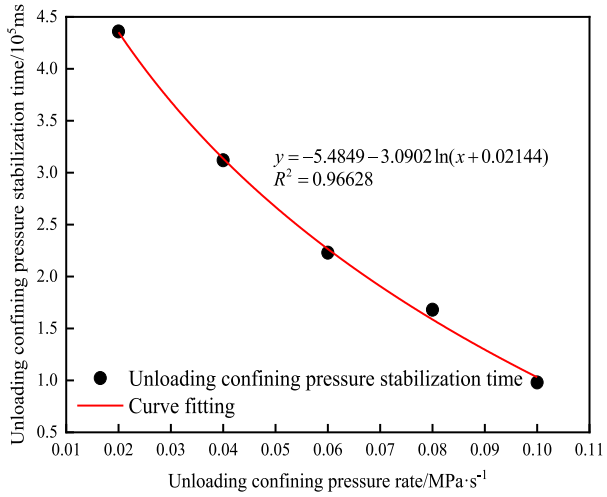

FIGURE 4
Unloading confining pressure stabilization time.

decreased by 18.84% compared to coal body with V_1 = 0.02 MPa/s. The confining pressure ratio of coal body with V_4 = 0.08 MPa/s decreased by 24.64% compared to coal body with V_1 = 0.02 MPa/s. The confining pressure ratio of coal body with V_5 = 0.1 MPa/s decreased by 28.99% compared to coal body with V_1 = 0.02 MPa/s.

3.3 Analysis of stability time of unloading confining pressure

Unloading stability time: The time taken from the start of unloading to the destruction of the sample. This value can be used as the early warning value of the failure time of the sample.

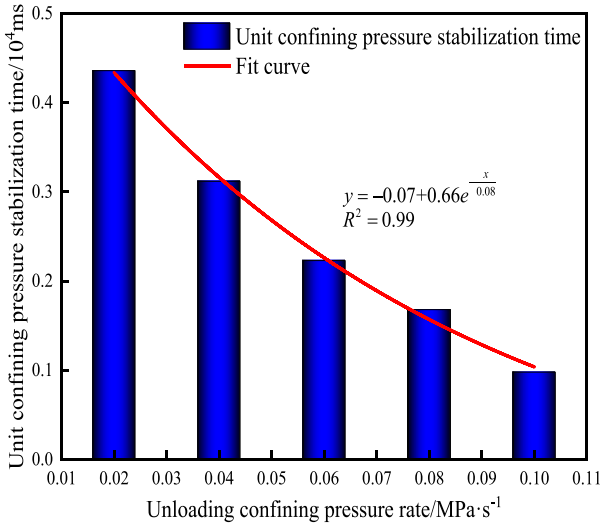

FIGURE 5
The time of unit confining pressure stability.

The time of unit confining pressure stability: the ratio of Unloading stability time to initial confining pressure. The trend of unloading stability time is shown in Figure 4. The time of unit confining pressure stability is shown in Figure 5.

It can be found from Figure 4 that as the unloading pressure rate increases, the unloading stability time of the coal sample decreases gradually; The stability time of coal samples at the rate of 0.04 mpa/s, 0.06 mpa/s, 0.08 mpa/s and 0.10 mpa/s is 25.44%, 48.85%, 61.47% and 77.52% less than that at the rate of 0.02 MPa/s respectively.

According to Figure 5, when the unloading pressure rate increases, the unit confining pressure stabilization time gradually decreases. It can be concluded that the stabilization time of the unloading confining pressure is longer when the rate of it is small, while the time is shorter when the rate of it is large. That is, the stability of the coal body under a low unloading pressure rate is better than that under a high rate. This is because of the internal crack of the coal body has sufficient time to expand and develop when the unloading pressure is low, so its damage will not happen suddenly. Otherwise, it would suddenly happen.

3.4 Strength characteristics of coal samples

According to The Mogi-Coulomb strength criterion, in the principal stress space, the following expression is satisfied:

$$\tau_{oct} = \frac{1}{3}\sqrt{(\sigma_1 - \sigma_3)^2 + (\sigma_1 - \sigma_2)^2 + (\sigma_2 - \sigma_3)^2} \quad (3)$$

In conventional triaxial unloading tests, the following relationship exists:

$$\sigma_2 = \sigma_3 \quad (4)$$

Bringing Eq. 4 into Eq. 3 yields:

$$\tau_{oct} = \sqrt{2}(\sigma_1 - \sigma_3)/3 \quad (5)$$

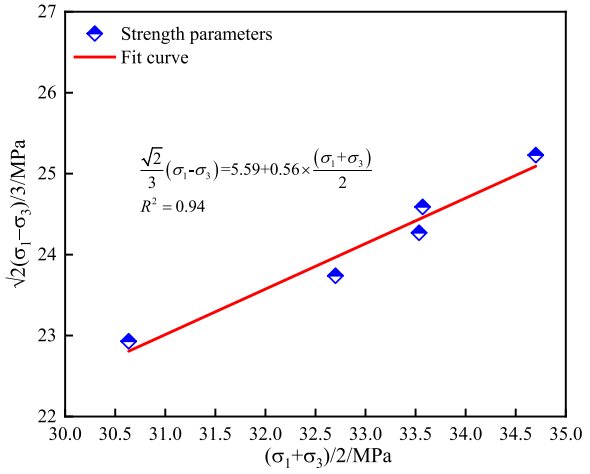

FIGURE 6
Strength characteristics of coal samples.

Assuming τ_{oct} and $\frac{\sigma_1+\sigma_3}{2}$ follow a linear relationship, then there is:

$$\tau_{oct} = a + \frac{b}{2}(\sigma_1 + \sigma_3) \tag{6}$$

Namely:

$$\frac{\sqrt{2}}{3}(\sigma_1 - \sigma_3) = a + \frac{b}{2}(\sigma_1 + \sigma_3) \tag{7}$$

Comparing the above relationship with the Mohr-Coulomb strength criterion, the relationship between the two is shown as follows:

$$a = \frac{2\sqrt{2}}{3} c \cos\phi \tag{8}$$

$$b = \frac{2\sqrt{2}}{3} \sin\phi \tag{9}$$

According to Eq. 7, perform regression analysis on the strength data of samples under different unloading rates, and the curve is shown in Figure 6.

From Figure 6, it can be found that the correlation degree of the Mogi-Coulomb criterion regression curve for unloading coal reaches 0.94, indicating that the Mogi-Coulomb criterion can better represent the strength characteristics of coal under conventional triaxial unloading paths. At the same time, according to Eqs 8, 9 and regression curve fitting parameters, it can be seen that the cohesion of coal under unloading paths is 7.37 MPa, and the internal friction angle is 36.45 °.

4 Energy evolution characteristics of coal body

4.1 Energy characteristics of coal body

During the experiment, a portion of the total energy of the coal body is converted into elastic energy and stored inside the sample, while the other portion is consumed in the form of dissipated energy during the evolution of the sample cracks (Du X. H. et al., 2022b; Du et al., 2023). The simplified formula for calculating the energy of each part of the coal sample is as follows:

$$U = \int_0^{\varepsilon_1} \sigma_1 d\varepsilon_1 + 2\int_0^{\varepsilon_3} \sigma_3 d\varepsilon_3 \tag{10}$$

$$U_e = \frac{\sigma_1^2}{2E_0} \tag{11}$$

$$U_d = U - U_e \tag{12}$$

In summary, the energy curve of the coal body is shown in Figure 7.

From Figure 7, it can be found that as the axial strain enlargement, the total energy value continuously increases. The elastic energy first increases to its maximum value and then begins to decrease. The dissipative energy first slowly increases, and then rapidly increases when cracks start to develop in large quantities.

Elastic stage: The cracks are not developed, so the dissipation energy is extremely low. The energy input in this stage is basically stored inside the coal body, so the total energy curve is similar to the elastic energy curve.

Plastic stage: The cracks begin to initiate and develop in large quantities, and the dissipative energy starts to rise. Part of the total energy is converted into elastic performance, while the other part is converted into dissipated energy. As the dissipated energy begins to increase, the increase in elastic performance decreases, causing the elastic energy curve to gradually move away from the total energy curve.

Post peak stage: At this stage, the stress has reached its maximum value, and its bearing capacity begins to reduce. The internal cracks of the coal body rapidly expand and form macroscopic cracks through each other. Therefore, the dissipated energy rose rapidly, while the elastic energy decreases rapidly.

4.2 Energy characteristics of coal body at peak stress points

The maximum stress is the maximum stress required for the coal body to reach failure, which can be considered as the turning point of failure for the entire experiment, as well as the turning point of changes in elastic energy and dissipative energy.

During loading, the stress value of the coal body rises continuously with the accumulation of strain. After the pre peak unloading begins, the stress value of the coal body will first try to rise by a certain amount, which is closely related to the unloading rate. When the maximum strength is reached, the stress value of the coal body begins to reduce, and the magnitude of the decrease is also greatly affected by the unloading rate. There are changes and transformations in energy during both loading and unloading of coal body. During the loading period, the experimental equipment and external input energy are more stored inside the coal sample, while a small portion of the energy is dissipated by the crack development of the coal body during the loading period; After unloading, due to a certain rise in the stress value of the coal body, most of the total energy is transformed into elastic performance. Moreover, due to the stress exceeding the yield stress during unloading, the cracks

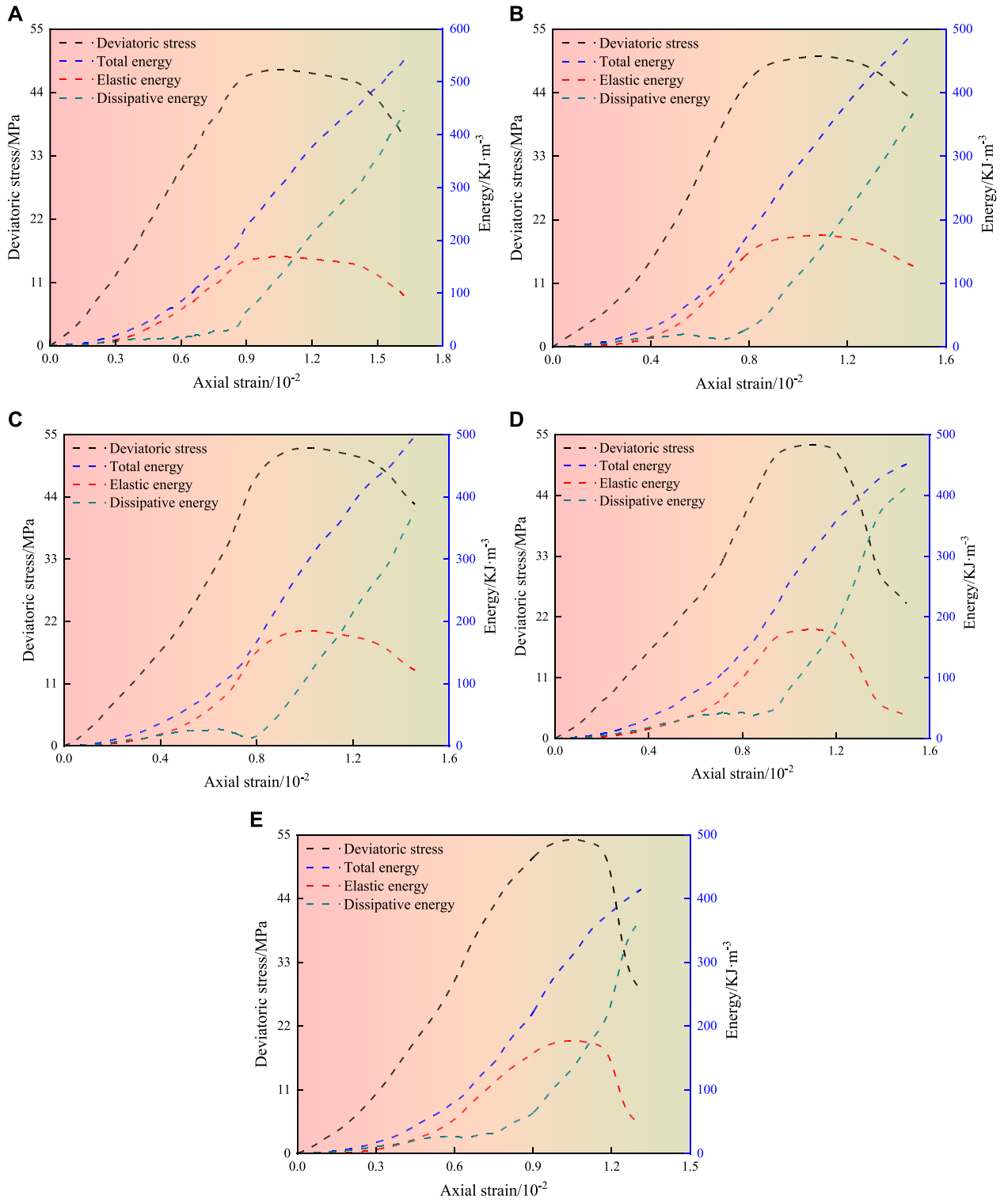

FIGURE 7
Energy characteristics of coal body: **(A)** V_1 = 0.02 MPa/s; **(B)** V_2 = 0.04 MPa/s; **(C)** V_3 = 0.06 MPa/s; **(D)** V_4 = 0.08 MPa/s; **(E)** V_5 = 0.1 MPa/s.

also start to initiate and develop in large quantities, resulting in an increase in dissipated energy, but it is less than the elastic performance. When the stress reaches the maximum stress, the stress state also reaches the required stress value for failure, and during the unloading period, as the circumferential constraint force decreases, the coal sample begins to rapidly deform and break. The input energy during this stage is largely consumed by the expansion of coal sample cracks, while the energy converted into elastic properties begins to decrease. And as the unloading time increases, the more elastic energy decreases.

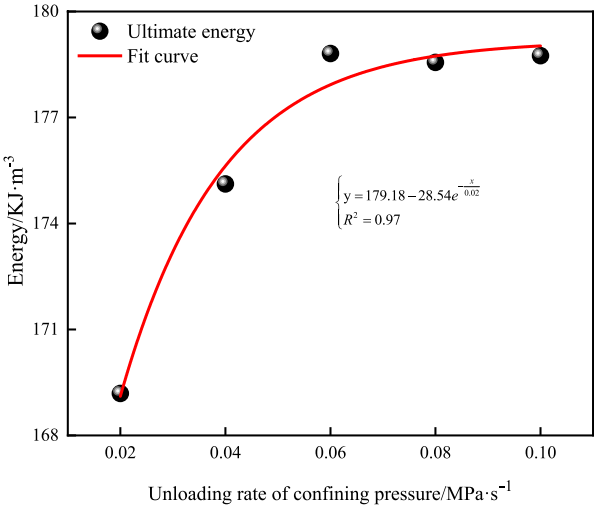

FIGURE 8
Trend of maximum elastic energy variation.

In summary, the peak point serves as the turning point of coal body failure, at the peak moment, the elastic energy of sample reaches its maximum value and is stored inside the coal body. When this value is exceeded, the bearing capacity of the coal body decreases, and the energy accumulated by the coal body exceeds its limit energy storage value, causing the coal body to be destroyed. Therefore, the ultimate energy storage value of coal body is necessary for studying the destruction of media. The maximum elastic energy under five unloading rates is shown in Figure 8.

From Figure 8, As the unloading rate increases, the ultimate elastic energy of the coal body maintains an increasing trend, but the increase amplitude is different. When the unloading rate is less than 0.06 MPa/s, the increase rate of the ultimate elastic energy of the coal body is relatively large. When the unloading rate is greater than 0.06 MPa/s, the increase rate of the ultimate elastic energy of the coal body decreases significantly and remains basically stable. Fitted the trend of changes between the two, the ultimate elastic energy of the coal body rises exponentially with the rise of unloading rate.

During excavation activities, stress concentration occurs around the mining area. This process allows the coal body to store a large amount of energy. When energy storage exceeds the limit that coal can withstand, it will suddenly be released, leading to dynamic disasters. According to the above analysis, When the unloading rate is high, the greater the ultimate elastic energy of the sample. In the actual mining process, a reasonable mining rate should be established to ensure that the surrounding coal masses are in a reasonable unloading state, which can avoid power disasters and ensure the safety of the working environment.

The coal and gas outburst accidents in deep high gas mines seriously threaten the safety of mine production and personal safety. The occurrence of mine power disasters is essentially the function of energy, and the unloading rate affects the conversion of coal energy. Hu and wen utilized research on the mechanical mechanism of coal and gas outburst to divide the outburst process into four stages: preparation, initiation, development, and termination. He believed that the three necessary conditions for outburst occurrence were the initial instability condition, the continuity of failure condition, and the energy condition (Zhang, 2022). The mechanical process is shown in Figure 9.

The higher the confining pressure, the higher the elastic modulus of the coal body, and the greater the elastic energy released during instability and failure. And the unloading of confining pressure during mining can lead to the deterioration of the strength of the coal body. However, after unloading begins, the decrease in confining pressure leads to an increase in the differential stress of the coal body. However, before unloading the confining pressure, the continuous energy input is converted into

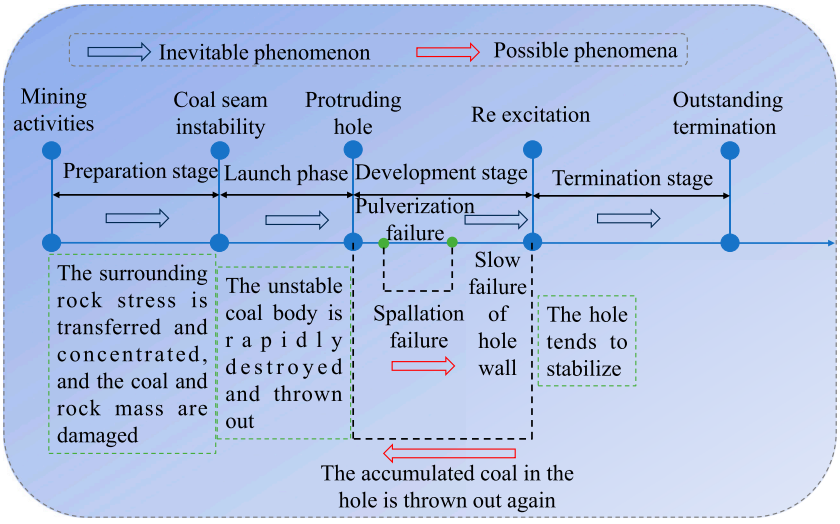

FIGURE 9
Mechanical process of coal and gas outburst.

elastic energy, and the sudden unloading of confining pressure causes the coal body to begin to expand, causing a large amount of energy to be converted into dissipated energy, which in turn causes the coal body to be rapidly damaged. Especially under the action of high unloading confining pressure rate, the failure of coal tends to be brittle, and the energy release rate is faster, which is easy to cause dynamic disasters.

5 Conclusion

(1) After unloading begins, the AE signal of the coal body varies at different unloading rates. The maximum stress and AE ringing count both rise exponentially with the rise of unloading confining pressure rate.
(2) Through analysis of the confining pressure, time, and confining pressure ratio during the unloading period of coal body, it was found that the higher the unloading rate, the easier and earlier the coal body is to be damaged.
(3) The dissipated energy of the coal sample in the elastic stage is extremely low, and a large amount of total energy was stored inside the coal sample. The dissipation energy increases during the plastic stage, while the trend of increasing elastic energy slows down. After the peak stage, the dissipated energy rapidly rises and the elastic energy reduces.
(4) Before unloading the confining pressure, the continuous energy input is converted into elastic energy, and the sudden unloading of confining pressure causes the coal body to begin to expand, causing a large amount of energy to be converted into dissipated energy, which in turn causes the coal body to be rapidly damaged. Especially under the action of high unloading confining pressure rate, the failure of coal tends to be brittle, and the energy release rate is faster, which is easy to cause dynamic disasters.

Data availability statement

The original contributions presented in the study are included in the article/Supplementary Material, further inquiries can be directed to the corresponding author.

Author contributions

JM: Conceptualization, Writing–original draft, Writing–review and editing. XJ: Data curation, Software, Validation, Funding acquisition, Writing–review and editing. SG: Project administration, Resources, Visualization, Writing–review and editing. XZ: Investigation, Methodology, Writing–review and editing. SC: Investigation, Project administration, Writing–review and editing. WZ: Conceptualization, Software, Writing–original draft.

Funding

The author(s) declare that financial support was received for the research, authorship, and/or publication of this article. This research was funded by the National key R&D Program of China, (Grant No. 2018YFC0808000), National Natural Science Foundation of China (Grant No. 51904013).

Conflict of interest

Author XJ was employed by Huaihe Energy Holding Group Co., Ltd. Authors SG, XZ, and SC were employed by Huaihe Energy Western Coal Power Group Co., Ltd. Author WZ was employed by Pingan Coal Mine Gas Control National Engineering Research Center Co., Ltd.

The remaining author declares that the research was conducted in the absence of any commercial or financial relationships that could be construed as a potential conflict of interest.

Publisher's note

All claims expressed in this article are solely those of the authors and do not necessarily represent those of their affiliated organizations, or those of the publisher, the editors and the reviewers. Any product that may be evaluated in this article, or claim that may be made by its manufacturer, is not guaranteed or endorsed by the publisher.

References

Chen, X. Z., He, J. D., Xiao, M. S., Xie, H. Q., and Liu, J. F. (2014). Dilatancy and energy properties of marble under triaxial unloading condition. *Chin. J. Geotech. Eng.* 36 (6), 1106–1112.

Chen, Y. L., Zuo, J. P., Liu, D. J., Li, Y. J., and Wang, Z. B. (2021). Experimental and numerical study of coal-rock bimaterial composite bodies under triaxial compression. *Int. J. Coal Sci. Techn* 8 (5), 908–924. doi:10.1007/s40789-021-00409-5

Chi, X. L., Yang, K., and Wei, Z. (2021). Breaking and mining-induced stress evolution of overlying strata in the working face of a steeply dipping coal seam. *Int. J. Coal Sci. Techn* 8 (4), 614–625. doi:10.1007/s40789-020-00392-3

Cong, Y., Wang, Z., Zheng, Y., Feng, X., and Zhang, L. (2016). Energy evolution principle of fracture propagation of marble with different unloading stress paths. *J. Cent. South Univ. Sci. Technol.* . 47 (9), 3140–3147.

Ding, Z. W., Jia, J. D., Tang, Q. B., and Li, X. F. (2022). Mechanical properties and energy damage evolution characteristics of coal under cyclic loading and unloading. *Rock Mech. Rock Eng.* 55 (8), 4765–4781. doi:10.1007/s00603-022-02884-x

Du, F., Ma, J., Guo, X. F., Wang, T. F., Dong, X. H., Li, J. S., et al. (2022a). Rockburst mechanism and the law of energy accumulation and release in mining roadway: a case study. *Int. J. Coal Sci. Techn* 9 (5), 67–17. doi:10.1007/s40789-022-00521-0

Du, X. H., Xue, J. H., Ma, Q., Chen, Z. H., and Zhan, K. L. (2022b). Energy evolution characteristics of coal–rock composite bodies based on unidirectional load. *Nat. Resour. Res.* 31 (3), 1647–1663. doi:10.1007/s11053-022-10039-6

Du, X. H., Xue, J. H., Shi, Y., Cao, C. R., Shu, C. M., Li, K. H., et al. (2023). Triaxial mechanical behaviour and energy conversion characteristics of deep coal bodies under confining pressure. *Energy* 266, 1–12. doi:10.1016/j.energy.2022.126443

Karim, K., and Yamazaki, F. (2001). Effect of earthquake ground motions on fragility curves of highway bridge piers based on numerical simulation. *Earthq. Eng. Struct. D.* 30 (12), 1839–1856. doi:10.1002/eqe.97

Li, D., Sun, Z., Li, X., and Xie, T. (2016). Mechanical response and failure characteristics of granite under different stress paths in triaxial loading and unloading conditions. *Chin. J. Geotech. Eng.* 35, 3449–3457. doi:10.13722/j.cnki.jrme.2016.0815

Li, D., Sun, Z., Xie, T., Li, X., and Ranjith, P. (2017a). Energy evolution characteristics of hard rock during triaxial failure with different loading and unloading paths. *Eng. Geol.* 228, 270–281. doi:10.1016/j.enggeo.2017.08.006

Li, H. T., Li, X. L., Fu, J. H., Zhu, N., Chen, D., Wang, Y., et al. (2023). Experimental study on compressive behavior and failure characteristics of imitation steel fiber concrete under uniaxial load. *Constr. Build. Mater* 399 (8), 132599. doi:10.1016/j.conbuildmat.2023.132599

Li, W., Lin, J., Shi, Z., Wen, J., Li, Y., Liu, Z., et al. (2019). Clomiphene citrate induces nuclear translocation of the tfeb transcription factor and triggers apoptosis by enhancing lysosomal membrane permeabilization. *Biochem Pharmacol.* 36 (1), 191–201. doi:10.1016/j.bcp.2018.11.016

Li, X., Chen, Z., Cao, W., Tao, M., and Zhou, J. (2017b). Time-effect properties and mechanisms of marble failure under different unloading rates. *Chin. J. Geotech. Eng.* 39 (9), 1565–1574.

Li, Y. L., Yang, R. S., Fang, S. Z., Lu, S. J., Zhu, Y., and Wang, M. S. (2022). Failure analysis and control measures of deep roadway with composite roof: a case study. *Int. J. Coal Sci. Techn* 9 (2), 2–18. doi:10.1007/s40789-022-00469-1

Liu, H. M., Li, X. L., Yu, Z. Y., Tan, Y., Ding, Y. S., Chen, D. Y., et al. (2023b). Influence of hole diameter on mechanical properties and stability of granite rock surrounding tunnels. *Phys. Fluids* 35 (6), 064121. doi:10.1063/5.0154872

Liu, K., Zhang, Q., Wu, G., Li, J., and Zhao, J. (2019). Dynamic mechanical and fracture behaviour of sandstone under multiaxial loads using a triaxial Hopkinson bar. *Rock Mech. Rock Eng.* 52 (7), 2175–2195. doi:10.1007/s00603-018-1691-y

Liu, K., and Zhao, J. (2021). Progressive damage behaviours of triaxially confined rocks under multiple dynamic loads. *Rock Mech. Rock Eng.* 54 (6), 3327–3358. doi:10.1007/s00603-021-02408-z

Liu, S., and Li, X. (2022). Experimental study on the effect of cold soaking with liquid nitrogen on the coal chemical and microstructural characteristics. *Environ. Sci. Pollut. R.* 30 (13), 36080–36097. doi:10.1007/s11356-022-24821-9

Liu, S. M., Sun, H. T., Zhang, D. M., Yang, K., Li, X. L., Wang, D. K., et al. (2023a). Experimental study of effect of liquid nitrogen cold soaking on coal pore structure and fractal characteristics. *Energy* 275 (7), 127470. doi:10.1016/j.energy.2023.127470

Liu, W. J., Y, K., Zhang, S., Zhang, Z. N., and Xu, R. J. (2022). Energy evolution and water immersion-induced weakening in sandstone roof of coal mines. *Int. J. Coal Sci. Techn* 9 (1), 1–14. doi:10.1007/s40789-022-00529-6

Lou, J. F., Gao, F. Q., Yang, J. H., Ren, Y. F., Li, J. Z., Wang, X. Q., et al. (2021). Characteristics of evolution of mining-induced stress field in the longwall panel: insights from physical modeling. *Int. J. Coal Sci. Techn* 8, 938–955. doi:10.1007/s40789-020-00390-5

Luo, D., Su, G., and He, B. (2019). True triaxial test on rockburst of granites with different water saturations. *Rock Soil Mech.* 40 (4), 1331–1340. doi:10.16285/j.rsm.2017.2432

Ma, D., Duan, H. Y., Zhang, J. X., and Bai, H. B. (2022). A state-of-the-art review on rock seepage mechanism of water inrush disaster in coal mines. *Int. J. Coal Sci. Techn* 9 (1), 50–28. doi:10.1007/s40789-022-00525-w

Ma, P., Zhou, Y., and Liu, C. (2019). Energy evolution characteristics of coal failure in triaxial tests under different unloading confining pressure rates. *Rock Soil Mech.* 40 (7), 2645–2652. doi:10.16285/j.rsm.2018.1086

Peng, R. D., Ju, Y., Wang, J. G., Xie, H. P., Gao, F., and Mao, L. T. (2015). Energy dissipation and release during coal failure under conventional triaxial compression. *Rock Mech. Rock Eng.* 48 (2), 509–526. doi:10.1007/s00603-014-0602-0

Qi, T. Y., Zhang, F., Pei, X. M., Feng, G. R., and Wei, H. r. (2022). Simulation research and application on response characteristics of detecting water-filled goaf by transient electromagnetic method. *Int. J. Coal Sci. Technol.* 9 (1), 17. doi:10.1007/s40789-022-00478-0

Su, G. S., Yan, S. Z., Yan, Z. F., Zhai, S. B., and Yan, L. B. (2019). Evolution characteristics of acoustic emission in rockburst process under true-triaxial loading conditions. *Rock Soil Mech.* 40 (5), 1673–1682. doi:10.16285/j.rsm.2017.2550

Wang, C., Zhou, H., and Wang, R. (2019). Failure characteristics of Beishan granite under unloading confining pressures. *Chin. J. Geotech. Eng.* 41 (2), 140–148.

Wang, H. W., Wang, Z. L., Jiang, Y. D., Song, J. Q., and Jia, M. N. (2022). New approach for the digital reconstruction of complex mine faults and its application in mining. *Int. J. Coal Sci. Technol.* 9 (1), 43. doi:10.1007/s40789-022-00506-z

Wang, X. Q., and Gao, F. Q. (2022). Triaxial compression behavior of large-scale jointed coal: a numerical study. *Int. J. Coal Sci. Techn* 9 (1), 76–95. doi:10.1007/s40789-022-00534-9

Xie, H. P., Peng, R. D., and Ju, Y. (2004). Energy dissipation of rock deformation and fracture. *Chin. J. Rock Mech. Eng.* 21, 3565–3570.

Xie, S. R., Wang, E., Chen, D. D., Li, H., Jiang, Z. S., and Yang, H. Z. (2022b). Stability analysis and control technology of gob-side entry retaining with double roadways by filling with high-water material in gently inclined coal seam. *Int. J. Coal Sci. Technol.* 9 (1), 52. doi:10.1007/s40789-022-00524-x

Xie, S. R., Wu, Y. Y., Chen, D. D., Liu, R. P., Han, X. T., and Ye, Q. C. (2022a). Failure analysis and control technology of intersections of large-scale variable cross-section roadways in deep soft rock. *Int. J. Coal Sci. Technol.* 9 (1), 19. doi:10.1007/s40789-022-00479-z

Yang, S. Q. (2016). Experimental study on deformation, peak strength and crack damage behavior of hollow sandstone under conventional triaxial compression. *Eng. Geol.* 213, 11–24. doi:10.1016/j.enggeo.2016.08.012

Yang, W., Zhang, Q., Chen, F., Li, W., Wang, J., He, R., et al. (2012). Analysis of unloading confining pressure rheological tests in different stress paths and model identification. *J. Cent. South Univ. Sci. Technol.* . 43 (5), 1885–1893.

Yin, G., Lu, J., Li, X., Liu, C., Li, M., and Ma, B. (2018). Stability and plastic zone characteristics of surrounding rock under true triaxial stress conditions. *J. China Coal Soc.* 43 (10), 2709–2717. doi:10.13225/j.cnki.jccs.2017.1637

Yin, G., Ma, B., Liu, C., and Li, M. (2019). Effect of loading and unloading rates on mechanical properties and energy characteristics of sandstone under true triaxial stress. *J. China Coal Soc.* 44 (2), 454–462. doi:10.13225/j.cnki.jccs.2018.0438

Zhang, F., Ma, G., and Feng, D. (2019). Hydraulic fracturing simulation test and fracture propagation analysis of large-scale coal rock under true triaxial conditions. *Rock Soil Mech.* 40 (5), 1890–1897. doi:10.16285/j.rsm.2018.0041

Zhang, J., Li, X., Qin, Q., Wang, Y., and Gao, X. (2023). Study on overlying strata movement patterns and mechanisms in super-large mining height stopes. *B Eng. Geol. Environ.* 82 (3), 142. doi:10.1007/s10064-023-03185-5

Zhang, L., Kan, Z. H., Zhang, C., and Tang, J. (2022). Experimental study of coal flow characteristics under mining disturbance in China. *Int. J. Coal Sci. Techn* 9 (5), 66–47. doi:10.1007/s40789-022-00533-W

Zhang, S. (2022). *Stress release characteristics of tectonic coal under the condition of unloading confining pressure and its influence on outburst*. China University of Mining and Technology. doi:10.27623/d.cnki.gzkyu.2022.002395

Zhao, G., Dai, B., Dong, L., and Yang, C. (2015). Experimental research on mechanical characteristics and strength criterion of rock of triaxial unloading tests under different stress paths. *Rock Soil Mech.* 36 (11), 3121–3127. doi:10.16285/j.rsm.2015.11.011

Zheng, Q., Li, J., Ji, W., Zhao, X., and Wang, Z. (2017). Influence of different unloading confining pressure rates on energy evolution of rock failure process. *J. Qingdao Univ. Technol.* 38 (6), 13–17.